

Fold Geometry

5.1

Introduction

This chapter describes methods for defining the geometry of folded surfaces in three dimensions and methods for projecting data along and within fold trends. Folds can be divided into domains where the shapes are cylindrical or conical, smoothly curved or planar. The geometries within domains are efficiently described in terms of the orientations and properties of fold axes, plunge lines, crest lines and trough lines. The relationship of these elements to bed attitudes has implications for bed thickness changes and the persistence of the folds along their trend.

5.2

Trend from Bedding Attitudes

The fold trend and plunge is a key element in making and confirming the grain in a map. The change in shape along plunge is given by the fold form, cylindrical or conical. A fold in a cylindrical domain continues unchanged along plunge, whereas a fold in a conical domain will die out along plunge. The trend, plunge, and style of a fold are determined from the bedding attitudes as plotted on stereograms or tangent diagrams. The use of the tangent diagram is emphasized here because of its practical value in separating cylindrical from conical folds and in characterizing the type of conical plunge. The bedding attitude data are collected from outcrop measurements or from dipmeters. Dip-domain style folds may combine both cylindrical and conical elements. If the data show too much scatter for the form to be clear, the size of the domain under consideration can usually be reduced until the domain is homogeneous and has a cylindrical or conical geometry.

5.2.1

Cylindrical Folds

A cylindrical fold is defined by the property that the poles to bedding all lie parallel to the same plane regardless of the specific cross-sectional shape of the fold (Fig. 5.1a). This property is the basis for finding the fold axis. On a stereogram the poles to bedding fall on a great circle (Fig. 5.1b). The pole to this great circle is the fold axis, known as the π axis when determined in this manner. The trend of a cylindrical fold is parallel to its axis. A cylindrical fold maintains constant geometry along its axis as long as the trend and plunge remain constant.

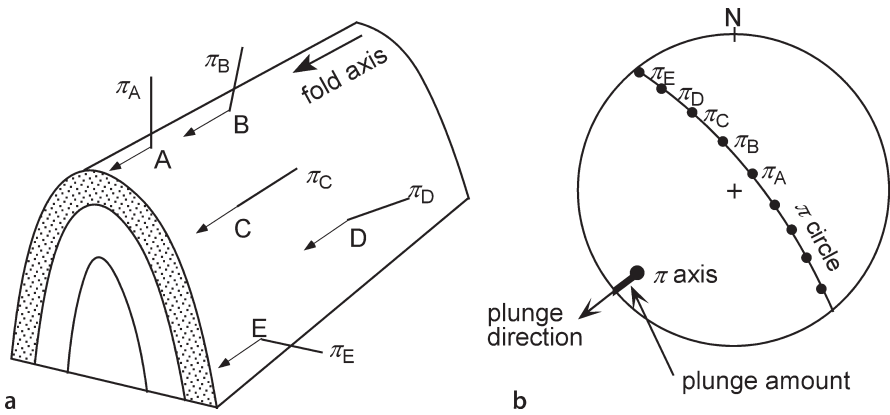
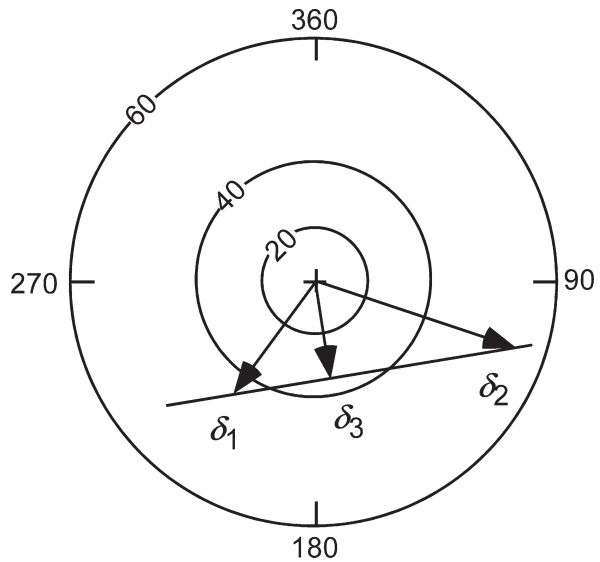


Fig. 5.1. Axis of a cylindrical fold. **a** Fold geometry. A–E are measurement points, π_A – π_E are poles to bedding. **b** Axis (π axis) determined from a stereogram, lower-hemisphere projection. (After Ramsay 1967)

Fig. 5.2.
Fold axis (δ_3) found as the intersection line between two bedding planes (δ_1 and δ_2) on a tangent diagram. (After Bengtson 1980)



The alternative method for finding the axis is to plot the bedding attitudes on a tangent diagram. The method is based on the principle that intersecting planes have the same apparent dip in a vertical plane containing their line of intersection (Bengtson 1980). Let δ represent the dip vector of a plane. In Fig. 5.2, planes δ_1 and δ_2 are plotted and connected by a straight line. The perpendicular to this line through the origin, δ_3 , gives the bearing and plunge of the line of intersection. In a cylindrical fold, all bedding planes intersect in the straight line (δ_3) which is the fold axis.

Each bedding attitude is plotted on the tangent diagram as a point at the appropriate azimuth and dip. If the best fit curve through the dip-vector points is a straight line,

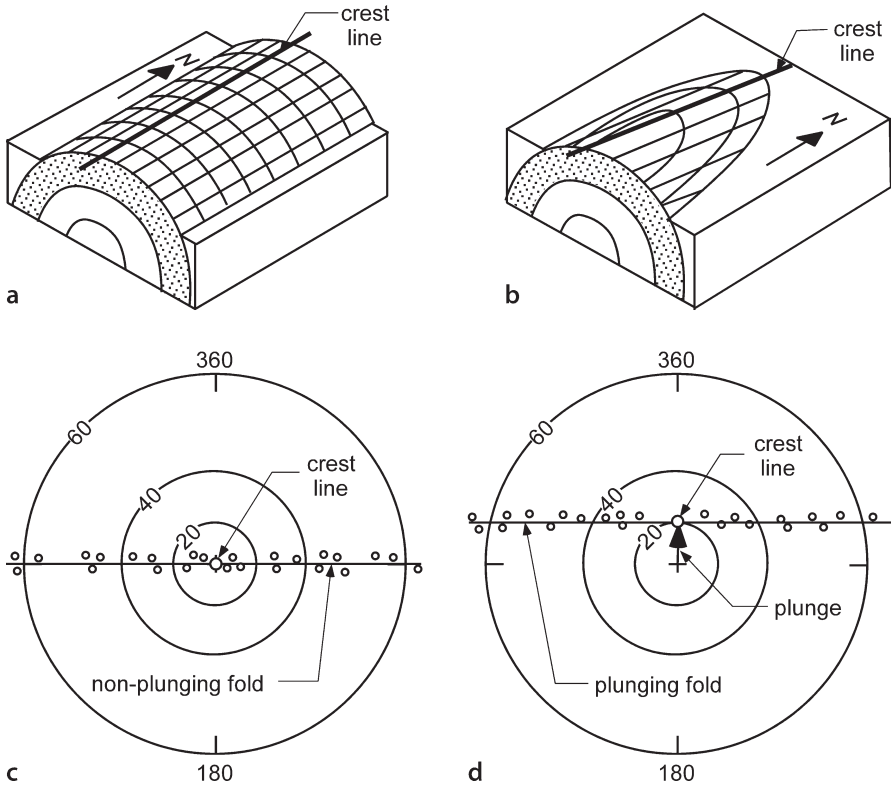


Fig. 5.3. Cylindrical folds showing trend and plunge of the crest line. **a** Non-plunging. **b** Plunging. **c** Tangent diagram of bed attitudes in a non-plunging fold. **d** Tangent diagram of bed attitudes in a plunging fold. (After Bengtson 1980)

the fold is cylindrical. The straight line through the dip vectors goes through the origin for a non-plunging fold (Fig. 5.3a,c) and is a straight line offset from the origin for a plunging fold (Fig. 5.3b,d). A vector from the origin to the line of dip vector points, perpendicular to the dip-vector line, that gives the bearing and plunge of the fold axis.

5.2.2

Conical Folds

A conical fold is defined by the movement of a generatrix line that is fixed at the apex of a cone (Fig. 5.4a); the fold shape is a portion of a cone. A conical fold terminates along its trend. On a stereogram the bedding poles fall on a small circle, the center of which is the cone axis and the radius of which is 90° minus the semi-apical angle (Fig. 5.4b). It is usually difficult to differentiate between cylindrical and slightly conical folds on a stereogram (Cruden and Charlesworth 1972; Stockmal and Spang 1982), yet this is an important distinction because a conical fold terminates along trend whereas a cylindrical fold does not. The tangent diagram is particularly good for making this distinction.

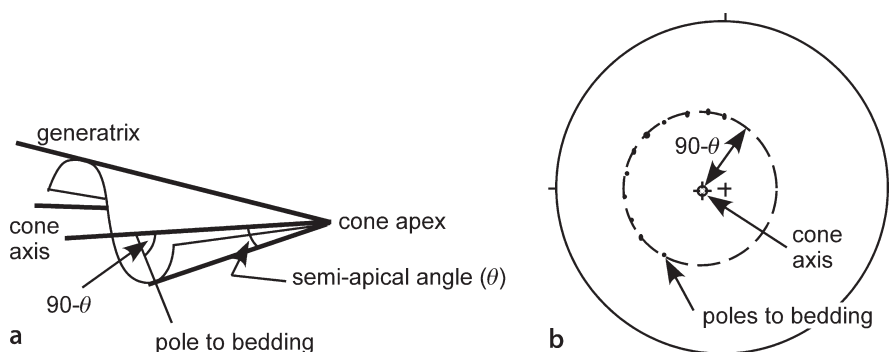


Fig. 5.4. Conical fold geometry. **a** Shape of a conically folded bed (after Stockmal and Spang 1982). **b** Lower-hemisphere stereogram projection of a conical fold (after Becker 1995)

On a tangent diagram, the curve through the dip vectors is a hyperbola (Bengtson 1980), concave toward the vertex of the cone. Type I plunge is defined by a hyperbola concave toward the origin. The fold spreads out and flattens down plunge (Fig. 5.5a,c). Type II plunge is defined by a hyperbola convex toward the origin on the tangent diagram (Fig. 5.5b,d) and the fold comes to a point down plunge. In the strict sense, a bed in a conical fold does not have an axis and therefore does not have a plunge like a cylindrical fold. The orientation of the crest line in an anticline (Fig. 5.5) or trough line in a syncline provides the line that best describes the orientation of a conically folded bed, in a manner analogous to the axis of a cylindrical fold. The plunge of a conical fold as defined on a tangent diagram is the plunge of the crest or trough line, not the plunge of the cone axis. If the crest line is horizontal, the fold is non-plunging but nevertheless terminates along the crest or trough. In general, each horizon in a fold will have its vertex in the same direction but at a different elevation from the vertices of the other horizons in the same fold.

The trend and plunge of the crest or trough of a conical fold is given by the magnitude the vector from the origin in the direction normal to the curve through the bedding dips (Figs. 5.6, 5.7). For points on the fold that are not on the crest or trough, the plunge direction is different. To find the plunge line, draw a line tangent to the curve at the dip representing the point to be projected. A line drawn from the origin, perpendicular to the tangent line gives the plunge amount and direction (Bengtson 1980). In a type I fold (Fig. 5.6), the minimum plunge angle is that of the crest line and all other plunge lines have greater plunge angles. In a type II fold (Fig. 5.7) the plunge line at some limb dip has a plunge of zero. The trend of this plunge line is normal to the tangent line (Fig. 5.7), the same as for all the other plunge lines. At greater limb dips in a type II fold, the down-plunge direction is away from the vertex of the cone (Fig. 5.7).

Because the tangent of 90° is infinity, a practical consideration in using a tangent diagram is that dips over 80° require an unreasonably large piece of paper. The non-linearity of the scale also exaggerates the dispersion at steep dips. A practical solution for folds defined mainly by dips under 80° is to plot dips over 80° on the 80° ring (Bengtson 1981b). This will have no effect on the determination of the axis and plunge of the folds (Bengtson 1981a,b) and will have the desirable effect of reducing the dis-

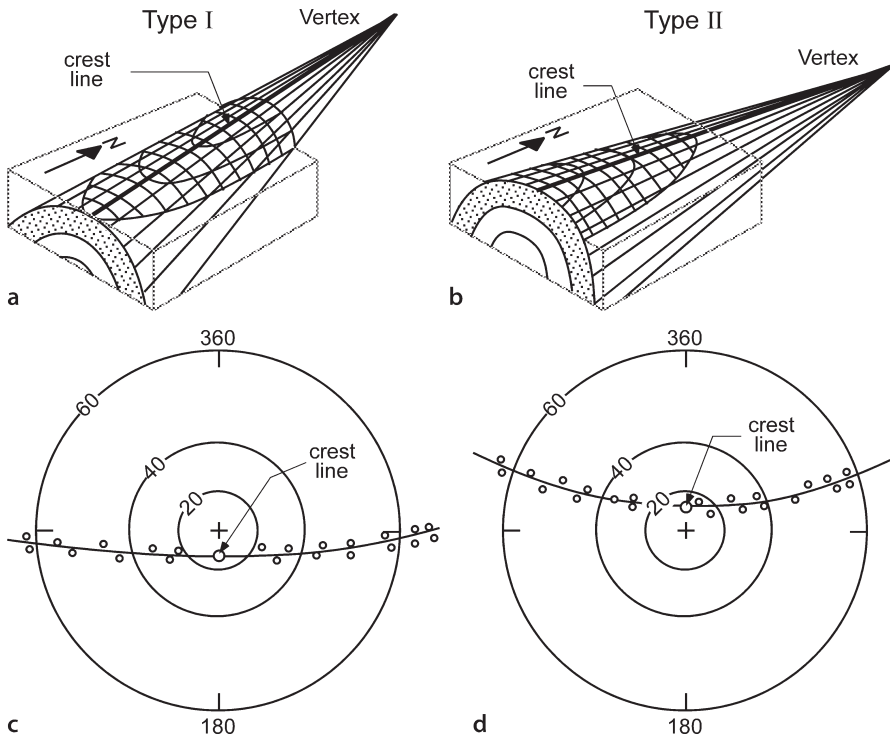
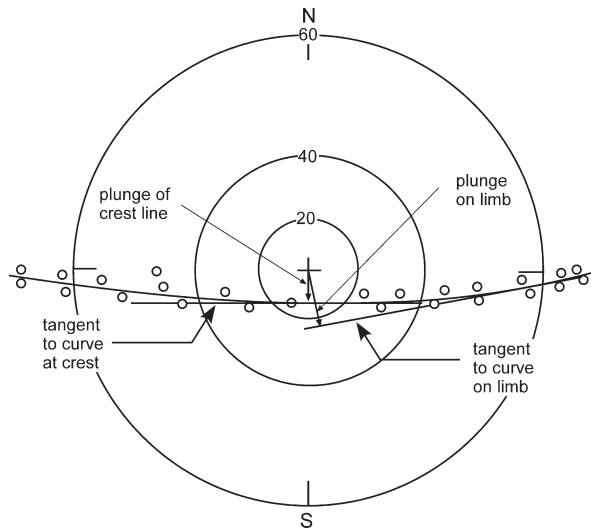


Fig. 5.5. Conical folds showing trend and plunge of crest line. **a** Type I plunge. **b** Type II plunge. **c** Tangent diagram of bed attitudes in a type I plunging fold. **d** Tangent diagram of bed attitudes in a type II plunging fold. (After Bengtson 1980)

Fig. 5.6.
Projection directions in a
type I conical fold



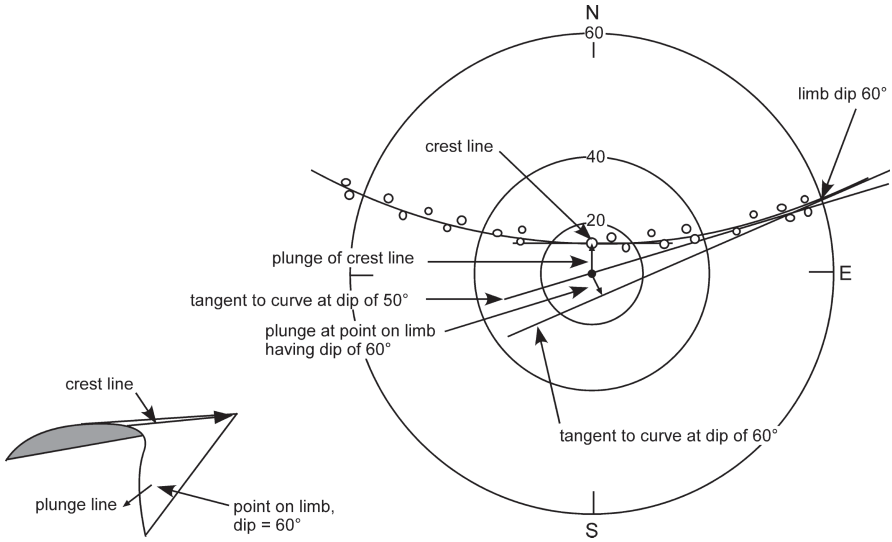


Fig. 5.7. Projection directions in a type II conical fold

persion of the steep dips. It is primarily the positions of the more gently dipping points that control the location of the axis and its plunge. The stereogram is the best method for fold axis determination for folds which contain mainly very steep dips.

5.2.3

Tangent Diagram on a Spreadsheet

Plotting dips on a tangent diagram is readily accomplished using a spreadsheet, which then allows the spreadsheet curve-fitting routines to be used to find the best-fit line or curve through the data. The following procedure allows a tangent diagram to be plotted as a simple xy graph on a spreadsheet. To place north (zero azimuth) at the top of the page, shift the origin with

$$Az = Az - 90 \quad , \quad (5.1)$$

where Az = azimuth of the dip. Change the dip magnitude to the tangent of the dip with

$$r = \tan(\delta) \quad , \quad (5.2)$$

where r = radius and δ = dip magnitude. Then change from polar to Cartesian coordinates with

$$x = r \cos Az \quad , \quad (5.3a)$$

$$y = r \sin Az \quad . \quad (5.3b)$$

The new coordinates than can plotted as an *xy* graph and will have the geometry of a tangent diagram. The best-fit curve through the data can be found with standard curve-fitting routines. Experience using simple spreadsheet curve-fitting functions indicates that when a quadratic curve produces a smooth hyperbolic-like shape (eg., Fig. 5.8b), it is an appropriate fit to the data. If a quadratic curve is irregular, then a straight-line best fit is more appropriate.

5.2.4

Example Using a Tangent Diagram

Attitude data from a traverse across the central part of the Sequatchie anticline (Fig. 5.8a) compiled in Table 5.1 provides an example of fold-axis determination using

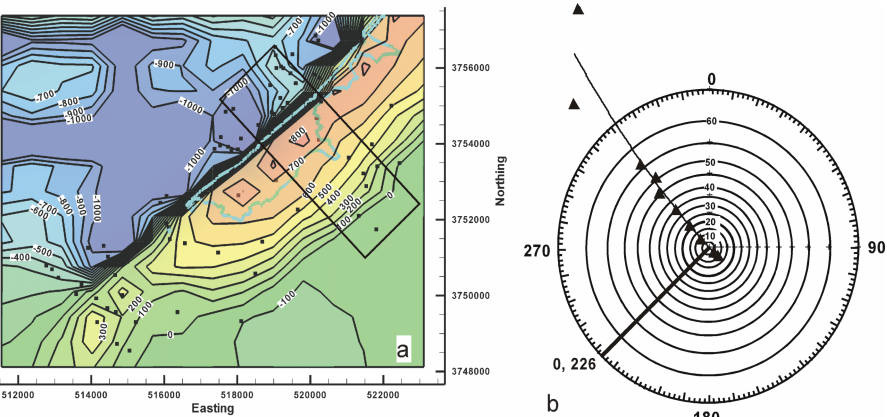


Fig. 5.8. Fold geometry of a portion of the Sequatchie anticline. **a** Index map to location of attitude data (*rectangle*) on structure-contour map. *Squares* represent measurement locations. **b** Tangent diagram for data within rectangle, showing best-fit curve through the data and the axis trend

Table 5.1.
Bedding attitudes across the central Sequatchie anticline from NW to SE

NW				SE	
Dip	Azimuth	Dip	Azimuth	Dip	Azimuth
8	308	56	318	6	144
46	315	75	330	8	145
34	316	83	315	8	144
50	320	70	315	6	127
6	320	0	000	7	136
22	316	5	145	10	136
				9	136

a tangent diagram. A preliminary plot of the data indicated that 83° dip attitude is inconsistent with the rest of the data and exerts too much control on the result, as mentioned above. Removing the 83° point results in a smooth best-fit curve that indicates a nonplunging fold with a slightly conical curvature, opening to the southwest and having a crestal trend of 0, 226 (Fig. 5.8b). This agrees with the geometry of the composite structure contour map (Fig. 5.8a).

5.2.5

Crest and Trough on a Map

A consistent definition of the fold trend, applicable to both cylindrical and conical folds, is the orientation of the crest or trough line (Fig. 5.9). In both cylindrical and conical folds (Figs. 5.3, 5.4) the crest line is a line on a folded surface along the structurally highest points (Dennis 1967). The trough line is the trace of the structurally lowest line. In cross section, the crest and trough traces are the loci of points where the apparent dip changes direction. In cylindrical folds the crest and trough lines are parallel to the fold axis and to each other, but in conical folds the crest and trough lines are not parallel. Crest and trough surfaces connect the crest and trough lines on successive horizons. The trace of a crest or trough surface is the line of intersection of the surface with some other surface such as the ground surface or the plane of a cross section. The crests and troughs of folds are of great practical importance because they are the positions of structural traps. Light fluids like most natural hydrocarbons will migrate toward the crests and heavy liquids will migrate toward the troughs.

The U-shaped trace of bedding made by the intersection of a plunging fold with a gently dipping surface, such as the surface of the earth, is called a fold nose. Originally a nose referred only to a plunging anticline (Dennis 1967; Bates and Jackson 1987) with a chute being the corresponding feature of a plunging syncline (Dennis 1967). Today, common usage refers to both synclinal and anticlinal fold noses. The term nose is also applied to the anticlinal or synclinal bend of structure contours on a single horizon (Fig. 5.9). The dip of bedding at the crest or trough line is the plunge of the line. The

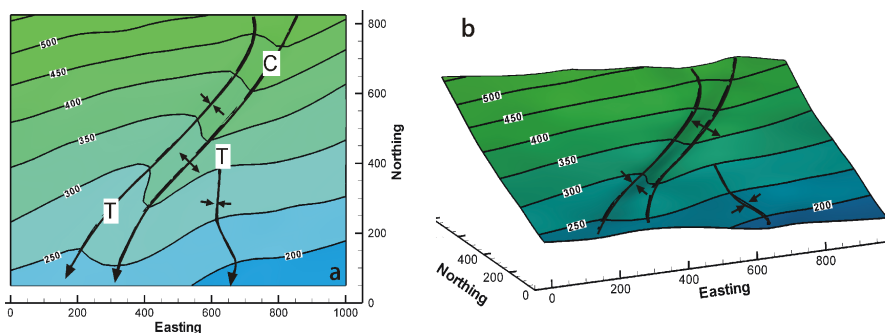


Fig. 5.9. Crest (C) and trough (T) lines on a structure contour map. **a** Plan view. Arrows point in the down-plunge direction. **b** 3-D oblique view to NE

spacing of structure contours along to the trend of the crest or trough gives the plunge of the crest or trough line:

$$\phi = \arctan (I/H) \quad , \quad (5.4)$$

where ϕ = plunge, I = contour interval, and H = map distance between the structure contours along the plunge.

5.3 Dip Domain Fold Geometry

A dip domain is a region of relatively uniform dip, separated from other domains by hinge lines or faults (Groshong and Usdansky 1988). Dip-domain style folding (Fig. 5.10) is rather common, especially in multilayer folds. A hinge line is a line of locally sharp curvature. On a structure contour map, hinge lines are lines of rapid changes in the strike of the contours. In a fixed-hinge model of fold development, the hinges represent the axes about which the folded layers have rotated.

The orientations of the hinge lines can be found using a stereogram by finding the intersection between the great circles that represent the orientations of the two adjacent dip domains (Fig. 5.11). If the intersection line is horizontal, as for hinge lines 1 and 2 in Fig. 5.10, the hinge line is not plunging. Hinge line 3 between the two dipping domains plunges 11° to the south (Fig. 5.11). The fold geometry between any two adjacent dip domains is cylindrical with the trend and plunge being equal to that of the hinge line. If the bed attitudes from multiple domains intersect at the same point on the stereogram, the fold is cylindrical, and the line is the fold axis, called the β -axis when determined this way (Ramsay 1967).

The tangent diagram (Fig. 5.12) shows the dip-domain fold from Fig. 5.10 to be conical with zero plunge. The concave-to-the-south curvature of the line through the dip vectors means that the fold terminates to the south, as observed (Fig. 5.10). If only the plunging nose of the fold is considered (Fig. 5.12), the hinge line is perpendicular to

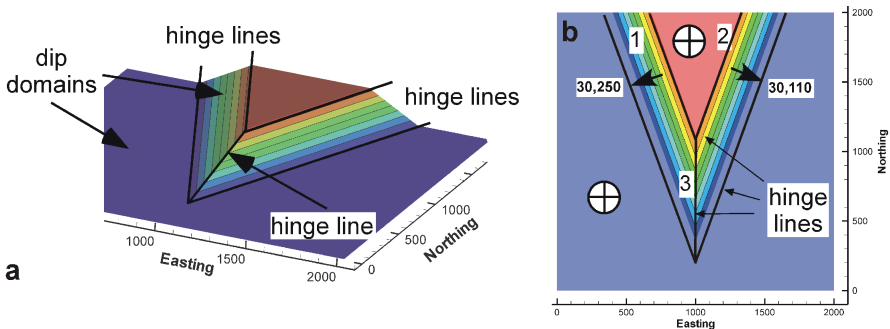


Fig. 5.10. Dip-domain fold (modeled after Faill 1973a). Hinge lines separate domains of constant dip. **a** 3-D oblique view to NW. **b** Bed attitudes and hinge lines (numbered), plan view

Fig. 5.11. Hinge line orientations for the fold in Fig. 5.10, found from the bed intersections on a lower-hemisphere equal-area stereogram. The primitive circle that outlines the stereogram is the trace of a horizontal bed. One of the bedding dip domains has an attitude of 30, 250 and the other of 30, 110. Numbered arrows give orientations of hinge lines. Hinge line 1 has the direction 0, 340; hinge line 2 is 0, 020; hinge line 3 is 11, 180

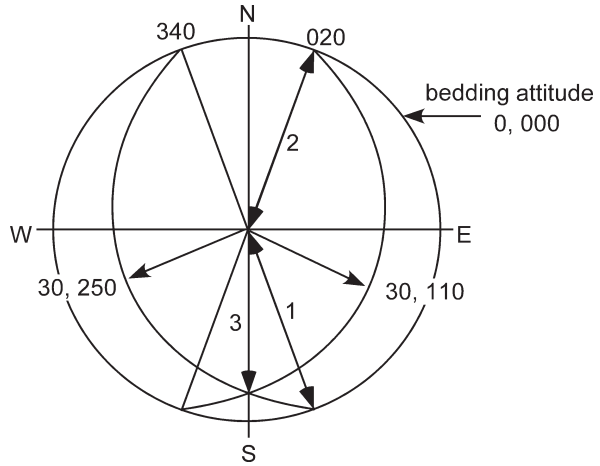
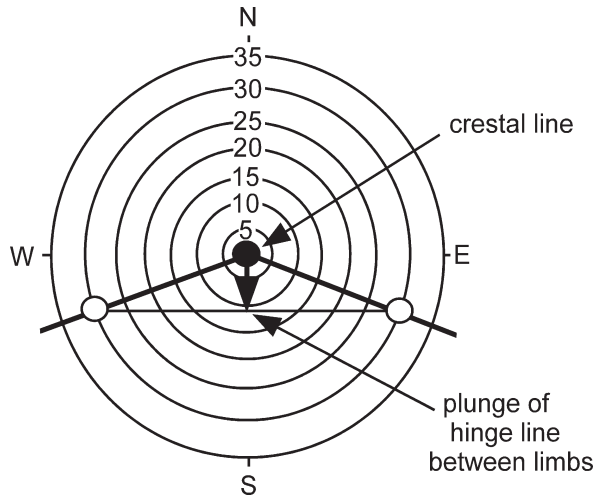


Fig. 5.12. Tangent diagram of the conical dip-domain fold in Fig. 5.10. Circles give attitudes of the three dip domains present in the fold



the straight line joining the two dip vectors (Fig. 5.12) and plunges 11° to the south, as observed (Figs. 5.10).

The analytical solution for the azimuth, θ' , and the plunge, δ , of a hinge line can be found as the line of intersection between the attitudes of two adjacent dip domains, from Eqs. 12.4, 12.5 and 12.29–12.31:

$$\theta' = \arctan(\cos \alpha / \cos \beta) \quad , \quad (5.5)$$

$$\delta = \arcsin(-\cos \gamma) \quad , \quad (5.6)$$

where

$$\cos \alpha = (\sin \delta_1 \cos \theta_1 \cos \delta_2 - \cos \delta_1 \sin \delta_2 \cos \theta_2) / N , \quad (5.7a)$$

$$\cos \beta = (\cos \delta_1 \sin \delta_2 \sin \theta_2 - \sin \delta_1 \sin \theta_1 \cos \delta_2) / N , \quad (5.7b)$$

$$\cos \gamma = (\sin \delta_1 \sin \theta_1 \sin \delta_2 \cos \theta_2 - \sin \delta_1 \cos \theta_1 \sin \delta_2 \sin \theta_2) / N , \quad (5.7c)$$

$$N = [(\sin \delta_1 \cos \theta_1 \cos \delta_2 - \cos \delta_1 \sin \delta_2 \cos \theta_2)^2 + (\cos \delta_1 \sin \delta_2 \sin \theta_2 - \sin \delta_1 \sin \theta_1 \cos \delta_2)^2 + (\sin \delta_1 \sin \theta_1 \sin \delta_2 \cos \theta_2 - \sin \delta_1 \cos \theta_1 \sin \delta_2 \sin \theta_2)^2]^{1/2} , \quad (5.8)$$

and the azimuth and plunge of the first plane is θ_1, δ_1 and of the second plane is θ_2, δ_2 . The value θ' given by Eq. 5.5 will be in the range of $\pm 90^\circ$ and must be corrected to give the true azimuth over the range of 0 to 360° . The true azimuth, θ , of the line can be determined from the signs of $\cos \alpha$ and $\cos \beta$ (Table 12.1). The direction cosines give a directed vector. The vector so determined might point upward. If it is necessary to reverse its sense of direction, reverse the sign of all three direction cosines. Note that division by zero in Eq. 5.5 must be prevented.

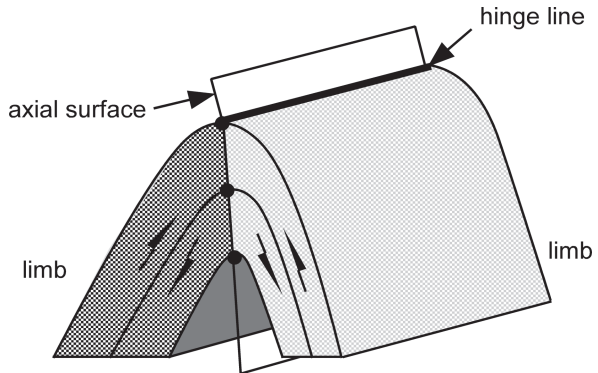
5.4 Axial Surfaces

The axial surface geometry is important in defining the complete three-dimensional geometry of a fold (Sect. 1.5) and in the construction of predictive cross sections (Sect. 6.4.1).

5.4.1 Characteristics

The axial surface of a fold is defined as the surface that contains the hinge lines of all horizons in the fold (Fig. 5.13; Dennis 1967). The axial trace is the trace of the axial surface on another surface such as on the earth's surface or on the plane of a cross section. The orientation of an axial surface within a fold hinge is related to the layer

Fig. 5.13. Characteristics that may be associated with an axial surface. The axial surface contains the hinge lines of successive layers (the defining property). The surface may be the boundary between fold limbs (different shading) and may be the plane across which the sense of layer-parallel shear (double arrows) reverses direction



thicknesses on the limbs. If, for example, the layers maintain constant thickness, the axial surface bisects the hinge. An axial surface may have one or both of the additional attributes: (1) it may divide the fold into two limbs (Fig. 5.13), and (2) it may be the surface at which the sense of layer-parallel shear reverses direction (Fig. 5.13). In a fold with only one axial surface, the axial surface necessarily divides the fold into two limbs; however, many folds have multiple axial surfaces, none of which bisect the whole fold (Fig. 5.14). The relationship between a fold hinge and the sense of shear on either side of it depends on the movement history of the fold. The movement history of a structure is called its kinematic evolution and a model for the evolution is called a kinematic model. According to a fixed-hinge kinematic model, the hinge lines are fixed to material points within the layer and form the rotation axes where the sense of shear reverses, as shown in Fig. 5.13. Other kinematic models do not require the sense of shear to change at the hinge (Fig. 5.14b).

Dip-domain folds commonly have multiple axial surfaces (Fig. 5.14) which form the boundaries between adjacent dip domains. These axial surfaces are not likely to have the additional attributes described in the previous paragraph. The folds are not split into two limbs by a single axial surface (except in the central part of Fig. 5.14a). In the fixed hinge kinematic model, the sense of shear does not necessarily change across an axial surface although the amount of shear will change (i.e., across axial surface 4, Fig. 5.14b). Horizontal domains may be unslipped and so an axial surface may separate a slipped from an unslipped domain (i.e., axial surfaces 2 and 3, Fig. 5.14b), not a change in the shear direction.

In the strict sense, a round-hinge fold does not have an axial surface because it does not have a precisely located hinge line. In a round-hinge fold it must be decided what aspect of the geometry is most important before the axial surface can be defined

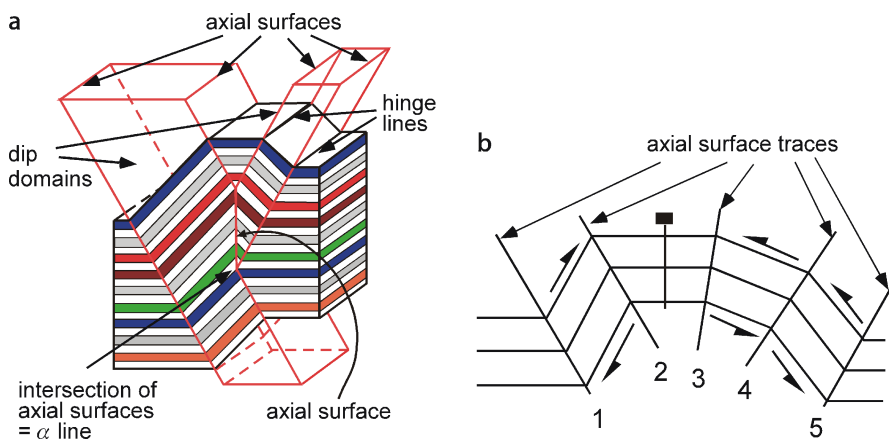


Fig. 5.14. Dip-domain folds. **a** Non-plunging fold showing hinge lines, axial surfaces, and axial surface intersection lines (modified from Faill 1969). Axial surface intersection lines are horizontal and parallel to the fold hinge lines. **b** Half arrows indicate the sense of shear in dipping domains. The horizontal domain does not slip, as indicated by the pin line. Axial surfaces are numbered

(Stockwell 1950; Stauffer 1973). For the purpose of describing the fold geometry, the virtual axial surface in a rounded fold is defined here as the surface which contains the virtual hinge lines. In relatively open folds, virtual hinge lines can be constructed as the intersection lines of planes extrapolated from the adjacent fold limbs (Fig. 5.15a). In a tight fold the extrapolated hinges are too far from the layers to be of practical use. In a tight fold (Fig. 5.15b) the virtual hinges can be defined as the centers of the circles (or ellipses) that provide the best fit to the hinge shapes, after the method of Stauffer (1973). Defined in this fashion, the axial surface divides the hinge into two limbs, but does not necessarily divide the fold symmetrically nor is it necessarily the surface where the sense of shear reverses. The axial surface, whether defined by actual or virtual fold hinges, does not necessarily coincide with the crest surface (Fig. 5.16) or the trough surface.

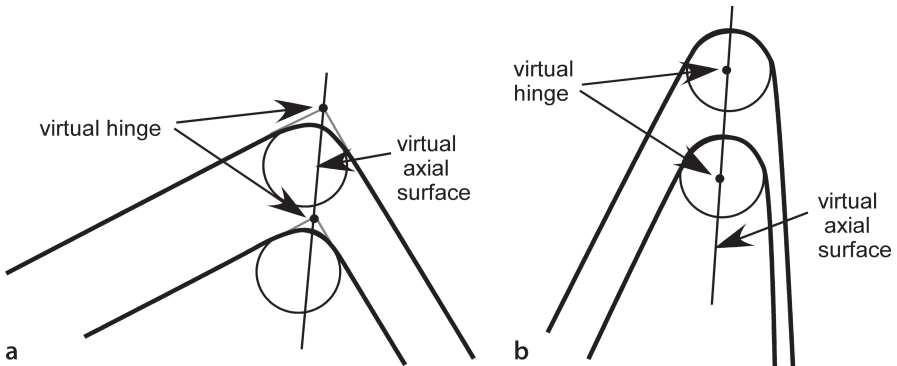
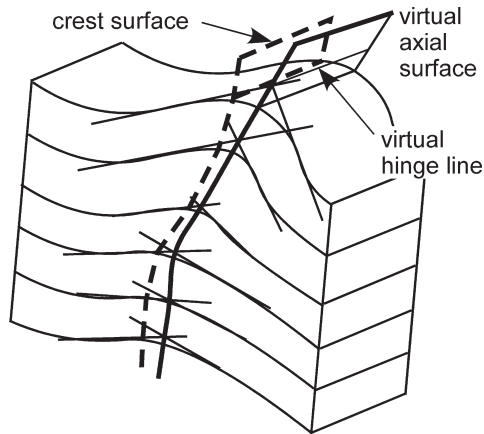


Fig. 5.15. Virtual hinges and virtual axial surfaces in cross sections of round-hinge folds. **a** Virtual hinges in an open fold found by extrapolating fold limbs to their intersection points. **b** Virtual hinges in a tight fold found as centers of circles tangent to the surfaces in the hinge. (After Stauffer 1973)

Fig. 5.16.
A fold in which the crest surface does not coincide with the axial surface



5.4.2 Orientation

Quantitative methods for the determination of the attitude of axial surfaces are given in this section. The orientation of an axial surface is related to the bed thickness change across it. In a cross section perpendicular to the hinge line, if a bed maintains constant thickness across the hinge, the axial surface bisects the hinge. The relationship between bed thickness and axial surface orientation is obtained as follows. Both limbs of the fold meet along the axial surface (Fig. 5.17) and have the common length h and therefore must satisfy the relationship

$$h = t_1 / \sin \gamma_1 = t_2 / \sin \gamma_2 \quad (5.9)$$

If $t_1 = t_2$, then $\gamma_1 = \gamma_2$ and the axial surface bisects the hinge (Fig. 5.17a). If the bed changes thickness across the axial surface, then the axial surface cannot bisect the hinge (Fig. 5.17b). The thickness ratio across the axial surface is

$$t_1 / t_2 = \sin \gamma_1 / \sin \gamma_2 \quad (5.10)$$

If the thickness ratio and the interlimb angle are known, then from the relationship (Fig. 5.17b)

$$\gamma = \gamma_1 + \gamma_2 \quad (5.11)$$

where γ = the interlimb angle and γ_2 = the angle between the axial surface and the dip of limb 2. Substitute $\gamma_1 = \gamma - \gamma_2$ from Eq. 5.11 into 5.10, apply the trigonometric identity for the sine of the difference between two angles, and solve to find γ_2 as

$$\gamma_2 = \arctan [t_2 \sin \gamma / (t_1 + t_2 \cos \gamma)] \quad (5.12)$$

The axial surface orientation in three dimensions can be found from a stereogram plot of the limbs. If the bed maintains constant thickness, the interlimb angle is bi-

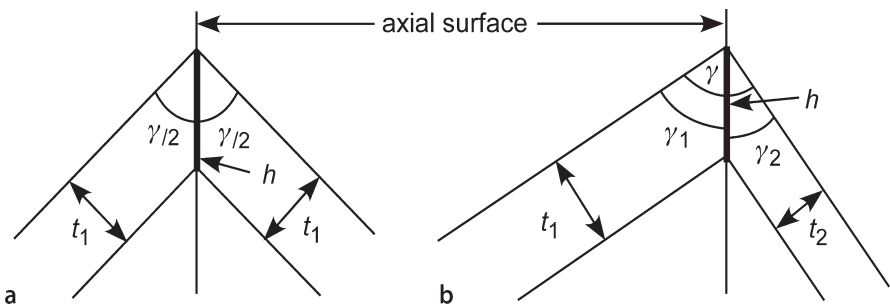


Fig. 5.17. Axial-surface geometry of a dip-domain fold hinge in cross section. **a** Constant bed thickness. **b** Variable bed thickness

sected. The bisector is found by plotting both beds (for example, 2 and H in Fig. 5.18), finding their line of intersection (I), and the great circle perpendicular to the intersection (*dotted line*). The obtuse angle between the beds is bisected by the double arrows. The great circle plane of the axial surface (shaded) goes through the bisection point and the line of intersection of the two beds. If bed thickness is not constant across the hinge, the partial interlimb angle is found from Eq. 5.12 and the appropriate partial angle is marked off along the great circle perpendicular to the line of intersection of the bedding dips.

Another method to determine the axial surface orientation is to find the plane through two lines that lie on the axial surface, for example, the trace of a hinge line on a map or cross section, and either the fold axis or the crest line (Rowland and Duebendorfer 1994). In the fold in Fig. 5.10, for example, hinge 3 plunges south and the surface trace of the hinge is north-south and horizontal and so the axial surface is vertical and strikes

Fig. 5.18. Determination of the axial surface orientation using a stereogram. Angle between two constant thickness domains, one horizontal (bed H) and one 30, 110 (bed 2). The axial surface (*shaded great circle*) bisects the angle (*double arrows*) between bed 2 and the horizontal bed. The axial surface attitude is 75, 290. Lower-hemisphere, equal-area projection

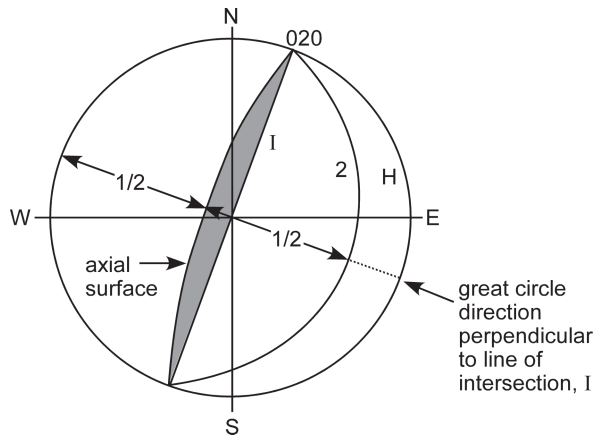


Fig. 5.19. Plunging dip-domain fold. The axial surface intersection lines (α) plunge in a direction opposite to that of the hinge line

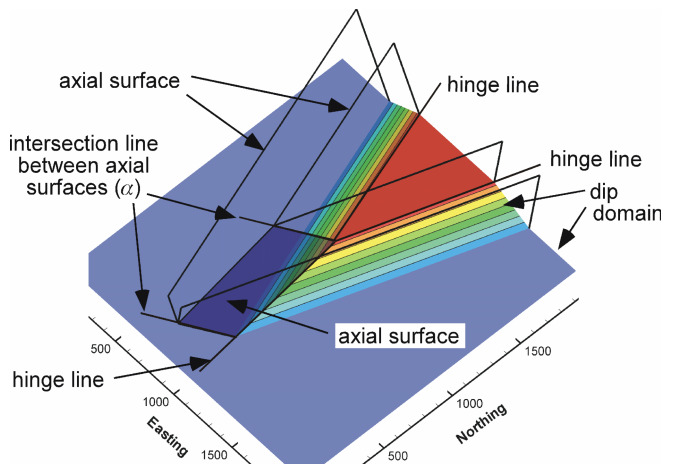
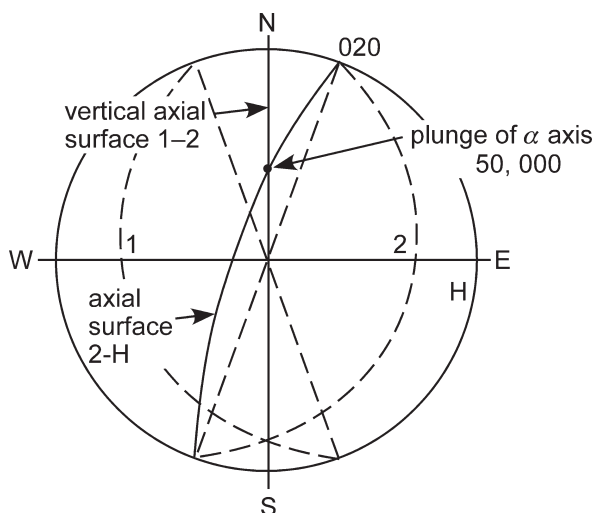


Fig. 5.20.

The intersection line between axial surfaces. Axial surface 1–2 bisects bed 1 (30,250) and bed 2 (30,110). Axial surface 2–H bisects bed 2 and bed H (0,000). The line of intersection of axial surfaces (50,000) is the α line. Lower-hemisphere, equal-area stereogram



north-south. In the general case, the axial trace and fold axis are plotted as points on the stereogram and the great circle that passes through both points is the axial surface. If the axial trace and the hinge line coincide, as is the case for hinges 1 and 2 in Fig. 5.10, this procedure is not applicable. It is then necessary to have additional information, either the trace of the axial surface on another horizon or the relative bed thickness change across the axial surface.

The intersection of two axial surfaces (Fig. 5.19) is an important line for defining the complete dip-domain geometry, and is here designated as the α line (α for axial surface). An α line has a direction and, unlike a fold axis, has a specific position in space. Angular folds may have multiple α lines. In a non-plunging fold an α line is coincident with a hinge line (Fig. 5.14a), but in a plunging fold (Fig. 5.19) the hinge lines and the α lines are neither parallel nor coincident.

The orientation of the α line is found by first finding the axial surfaces, and then their line of intersection. The stereogram solution is to draw the great circles for both axial surfaces and locate the point where they cross (Fig. 5.20), which is the orientation of the line of intersection. The analytical solution for the α line is that for the line of intersection between two planes (Eqs. 5.5–5.8), in which the two planes are axial surfaces.

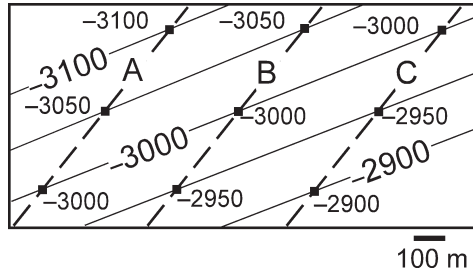
5.4.3

Location in 3-D

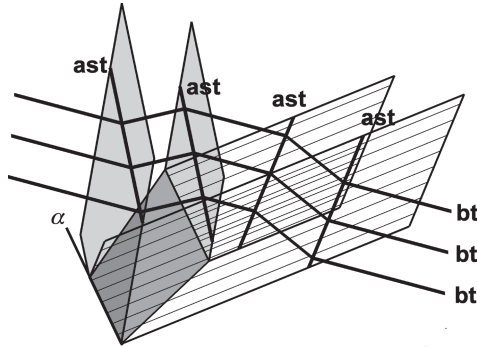
For a 3-D interpretation the axial surfaces and the α lines must be located in space as well as in orientation. If hinge lines are known from more than one horizon they can be combined to create a map (Fig. 5.21). The axial surface is the structure contour map of equal elevations on the hinge lines.

Fig. 5.21.

Structure contour map of an axial surface. *Dashed lines* are hinge lines on three different horizons, A, B, and C. *Solid lines* are contours on the axial surface. Contours are in meters

**Fig. 5.22.**

3-D axial surface geometry for the fold in Fig. 5.19. The axial surfaces bounding the left limb and the domain-intersection surface (bounded by α lines) are shaded, those bounding the right limb are indicated by their structure contours. The *heavy lines* represent a vertical slice through the structure: *ast*: axial surface trace; *bt*: bedding trace



Axial traces can be determined from cross sections, and then mapped to form a surface (Fig. 5.22). The cross sections may cross the structure in any direction and need not be normal to the axial surfaces. In 3-D software, the axial traces can be extracted from successive sections and these lines triangulated to form the axial surface. Having multiple beds on the cross sections makes choosing the trace straightforward. If only one horizon has been mapped, axial traces can still be inferred but then the section must be normal to the hinge line and the effect of thickness changes must be considered.

5.5

Using the Trend in Mapping

It may be necessary to know the fold trend before a reasonable map of the surface can be constructed. Elevations of the upper contact of a sandstone bed are shown in Fig. 5.23a. Preliminary structure contours, found by connecting points of equal elevation, suggest a northwest-southeast trend to the strike. There is nothing in the data in Fig. 5.23a to definitively argue against this interpretation. Given the knowledge that the fold trends north-south with zero plunge, the map of Fig. 5.23b can be constructed. It can now be seen that the original map connected points on opposite sides of the anticline. The correct structure of the map area could not be determined without knowing the fold trend.

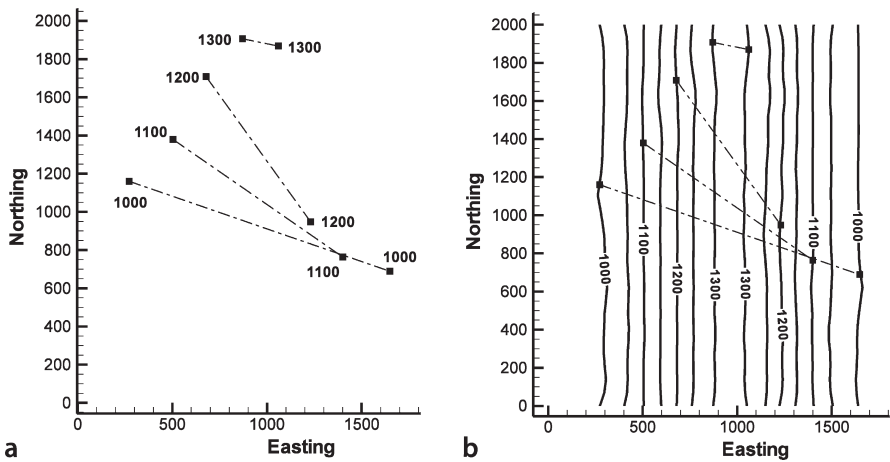


Fig. 5.23. Alternative structure contour maps from the same data. **a** Control points contoured. **b** Structure contours based on interpretation that the structure is a north-south trending, non-plunging anticline. Contours from **a** are dashed

5.6 Minor Folds

Map-scale folds may contain minor folds that can aid in the interpretation of the map-scale structure. The size ranking of a structure is the *order* of the structure. The largest structure is of the first-order and smaller structures have higher orders. Second- and higher-order folds are particularly common in map-scale compressional and wrench-fault environments. The bedding attitudes in the higher-order folds may be highly discordant to the attitudes in the lower-order folds (Fig. 5.24). Minor folds provide valuable information for interpreting the geometry of the first-order structure but, if unrecognized, may complicate or obscure the interpretation. A pitfall to avoid is interpreting the geometry of the first-order fold to follow the local bedding attitudes of the minor folds.

If produced in the same deformation event, the lower-order folds are usually coaxial or nearly coaxial to the first-order structure and are termed parasitic folds (Bates and Jackson 1987). Plots of the bedding attitudes of the minor folds on a stereogram or tangent diagram should be the same as the plots for the first-order structures and can be used to infer the axis direction of the larger folds. Seemingly discordant bedding attitudes seen on a map can be inferred to belong to minor folds if they plot on the same trend as the attitudes for the larger structure.

Asymmetric minor folds are commonly termed drag folds (Bates and Jackson 1987). A drag fold is a higher-order fold, usually one of a series, formed in a unit located between stiffer beds; the asymmetry is inferred to have been produced by bedding-parallel slip of the stiffer units. The sense of shear is indicated by the arrows in Fig. 5.24 and produces the asymmetry shown. The asymmetry of the drag folds can be used to infer the sense of shear in the larger-scale structure. In buckle folds, the sense of shear is away from the core of the fold and reverses on the opposite limbs of a fold (Fig. 5.24),

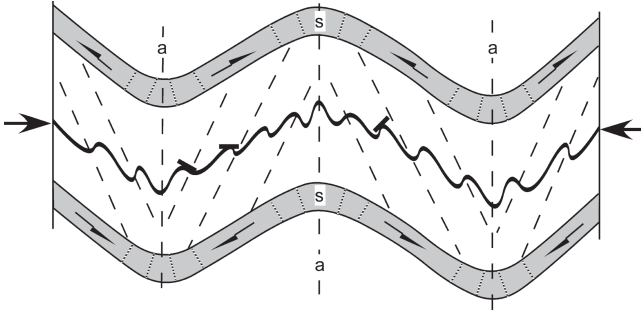


Fig. 5.24. Cross section of second-order parasitic folds in a thin bed showing normal (buckle-fold) sense of shear (*half arrows*) on the limbs of first-order folds. *Short thick lines* are local bedding attitudes. *Dashed lines labeled a* are axial-surface traces of first-order folds. *Unlabeled dashed lines* are cleavage, fanning in the stiff units (*s*) and antifanning in the soft units. *Large arrows* show directions of boundary displacements

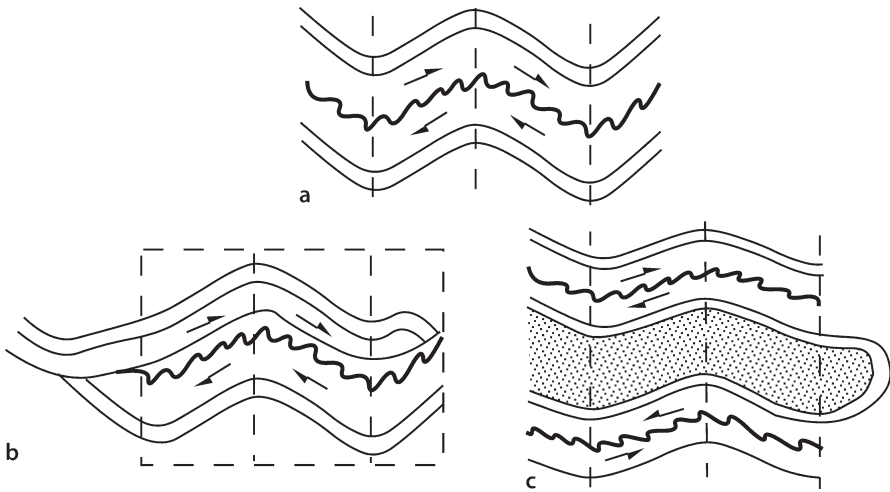


Fig. 5.25. Interpretations of drag folds having the same sense of shear on both limbs of a larger fold. **a** Observed fold with vertical axial traces. **b** Sense of shear interpreted as caused by a folded bedding-parallel thrust fault. **c** Sense of shear interpreted as being the upper limb of a refolded recumbent isoclinal fold

thereby indicating the relative positions of anticlinal and synclinal hinges. The inclination of cleavage planes in the softer units (Fig. 5.24), in the orientation axial planar to the drag folds, gives the same sense of shear information. Cleavage in the stiffer units is usually at a high angle to bedding, resulting in cleavage dips that fan across the fold.

Individual asymmetric higher-order folds are not always drag folds. The asymmetry may be due to some local heterogeneity in the material properties or the stress field, and the implied sense of shear could be of no significance to the larger-scale structure. Three or more folds with the same sense of overturning in the same larger

fold limb are more likely to be drag folds than is a single asymmetric fold among a group of symmetric folds.

Folds in which the sense of shear of the drag folds remains constant from one fold limb to the next (Fig. 5.25a) require a different interpretation. One possibility is the presence of a bedding-plane fault with transport from left to right (Fig. 5.25b); the folds would be fault-related drag folds. Alternatively the beds may be recumbently folded and then refolded with a vertical axial surface. In this situation (Fig. 5.25c), the sense of shear would be interpreted as in Fig. 5.24, and Fig. 5.25a then represents the upright limb of a recumbent anticline, the hinge of which must be to the right of the area of Fig. 5.25a, as shown in Fig. 5.25c.

Fold origins other than by buckling may yield other relationships between the sense of shear given by drag folds and position within the structure. Structures caused by differential vertical displacements, for example salt domes or gneiss domes, could result in exactly the opposite sense of shear on the fold limbs from that in buckle folds (Fig. 5.26). The pattern in Fig. 5.26 has been called Christmas-tree drag.

Fig. 5.26. Cross section of parasitic drag folds in the center bed as related to first-order differential vertical folding. Large arrows show directions of the boundary displacements

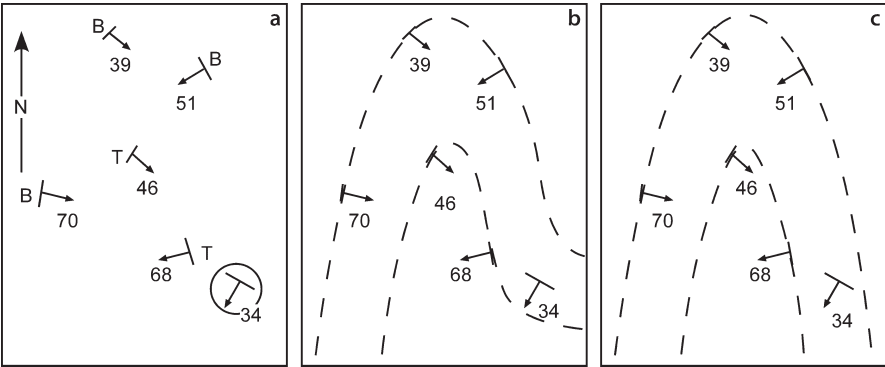
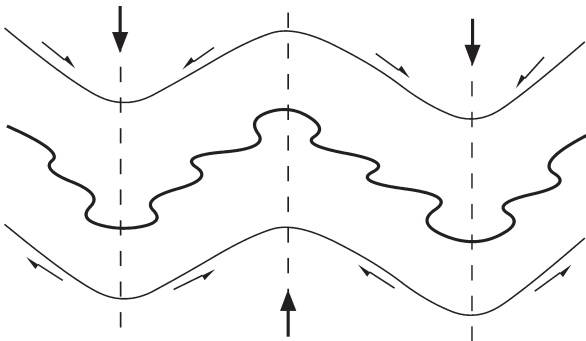


Fig. 5.27. Geological data and different possible geometries based on alternative interpretations of the significance of the *circled* attitude measurement. **a** Data. Bedding attitudes with *B*: observed base of formation; *T*: observed top of formation. **b** Interpretation honoring all contacts and attitudes. **c** Interpretation honoring all contacts but not all attitudes

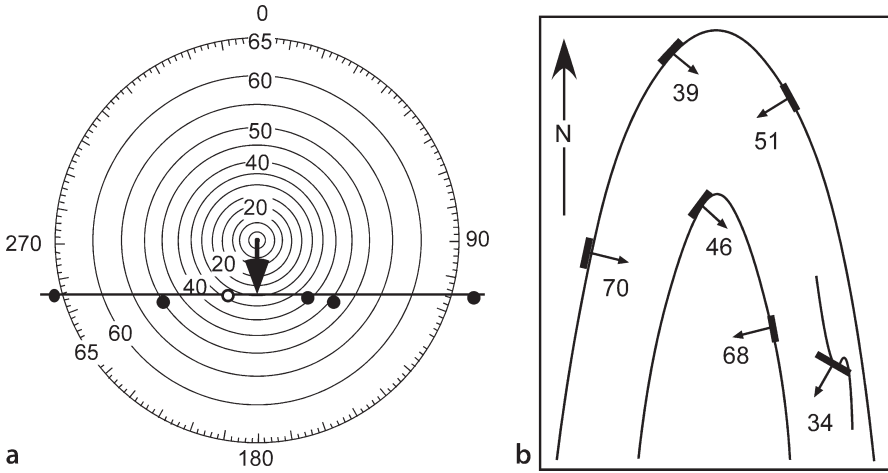


Fig. 5.28. Alternative interpretation of geological data in Fig. 5.27a. **a** Tangent diagram of bedding attitudes. *Open circle* is the 34, 212 point. Plunge of the fold is 30S. **b** Geological map of syncline with a coaxial minor fold on the limb. (After Stockwell 1950)

Potential interpretation problems associated with minor folds are illustrated by the map in Fig. 5.27a. The observed contact locations and bedding attitudes could be explained by the maps in either Fig. 5.27b or 5.27c. The shape of the first-order fold honors the 34SW dip in Fig. 5.27b and ignores it in Fig. 5.27c. The dip oblique to the contact could be justified as being either a cross bed or belonging to a minor fold.

Plotting the data from Fig. 5.27 on a tangent diagram (Fig. 5.28a) shows that all the points, including the questionable point (34, 212), fall on the same line, indicating a cylindrical fold plunging 30° due south. This result leads to rejection of the cross-bed hypothesis and indicates that the oblique bedding attitude is coaxial with the map-scale syncline. If the map of Fig. 5.27c is supported by the contact locations, then the structure has the form given by Fig. 5.28b.

5.7 Growth Folds

A growth fold develops during the deposition of sediments (Fig. 5.29a). The growth history can be quantified using an expansion index diagram, where the expansion index, E , is

$$E = t_d / t_u \quad , \quad (5.13)$$

with t_d = the downthrown thickness (off structure) and t_u = the upthrown thickness (on the fold crest). The thicknesses should be measured perpendicular to bedding so as not to confuse dip changes with thickness changes (Fig. 5.29a). The expansion index given here is the same as for growth faults (Thorsen 1963; Sect. 7.6). Different but related equations for folds have been given previously by Johnson and Bredeson (1971) and Brewer

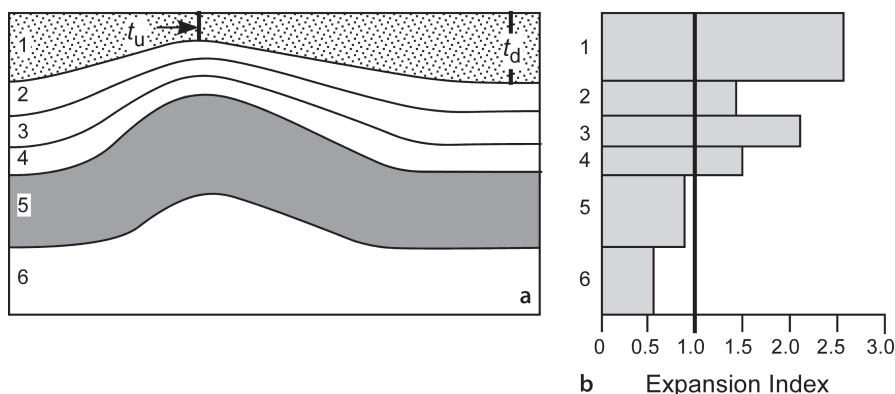


Fig. 5.29. Expansion index for a fold. Units 1–4 are growth units and units 5–6 are pre-growth units. **a** Cross section in the dip direction. **b** Expansion index diagram

and Groshong (1993). Using the same equation for both folds and faults facilitates the comparison of growth histories of both types of structures where they occur together.

The magnitude of the expansion index is plotted against the stratigraphic unit to give the expansion index diagram (Fig. 5.29b). The diagram illustrates the growth history of the fold. An expansion index of 1 means no growth and an index greater than 1 indicates upward growth of the anticlinal crest during deposition. The fold in Fig. 5.29a is a compressional detachment fold (Fig. 11.37) in which tectonic thickening in the pre-growth interval causes the expansion index to be less than 1. The growth intervals show an irregular upward increase in the growth rate. An expansion index diagram is particularly helpful in revealing subtle variations in the growth history of a fold and in comparing the growth histories of different structures. The expansion index is most appropriate for the sequences that are completely depositional. If erosion has occurred across the crest of the fold the expansion index will be misleading.

5.8 Exercises

5.8.1 Geometry of the Sequatchie Anticline

Plot the attitude data from Table 5.1 on a stereogram and on a tangent diagram to find the fold style and plunge. How do the two methods compare?

5.8.2 Geometry of the Greasy Cove Anticline

The bedding attitudes below (Table 5.2) come from the Greasy Cove anticline, a compressional structure in the southern Appalachian fold-thrust belt. What is the π axis of the fold? Use a tangent diagram to find the axis and the style of the fold.

Table 5.2.
Bedding attitudes, Greasy Cove
anticline, northeastern Alabama

Dip	Azimuth	Dip	Azimuth	Dip	Azimuth
46	316	55	316	60	310
55	311	40	295	14	124
12	319	26	281	60	304
20	248	25	275	10	270
10	266	14	294	16	307
12	243	15	173	12	150
24	154	22	154	28	231
20	129	30	128	30	119
35	143	25	114	32	131
25	120	70	151	26	165
20	345	12	255	11	258
15	160	12	190		

5.8.3
Structure of a Selected Map Area

Use the map of a selected structure (for example, Fig. 3.3 or 3.29) to answer the following questions. Measure and list all the bedding attitudes on the map. Plot the attitudes on a stereogram and a tangent diagram. What fold geometry is present? Which diagram gives the clearest result? Explain. Define the locations of the crest and trough traces from the map. Are the directions the same as given by the attitude diagrams? Find the attitudes of the axial planes, and locate the axial-plane traces on the map. What method did you use and why? What are the problems, if any, with the interpretation? Do the axial-surface traces coincide with the crest and trough traces? What are the orientations of the axial-surface intersection lines? Show where these intersection lines pierce the outcrop.

